doi:10.1017/S1431927622009552
Microsc. Microanal. 28 (Suppl 1), 2022

Objective Point Symmetry Classifications/Quantifications of an Electron Diffraction Spot Pattern with Pseudo-Hexagonal Lattice Metric

Peter Moeck[1*] and Lukas von Koch[1,2]

[1] Department of Physics, Portland State University, Portland, Oregon, USA
[2] Westside Christian High School, Portland, Oregon, USA
* Corresponding author: pmoeck@pdx.edu

The recently developed information-theoretic approach to crystallographic symmetry classifications and quantifications [1-4] in two dimensions (2D) from digital transmission electron and scanning probe microscope images is adapted here for the analysis of an experimental electron diffraction spot pattern, Fig. 1. Digital input data are in [1-3] considered to consist of the pixel-wise sums of approximately Gaussian distributed noise and an unknown underlying signal that is strictly 2D periodic. Structural defects within the crystals or on the crystal surfaces, instrumental image recording noise, slight deviations from zero-crystal-tilt conditions in transmission electron microscopy, and small inaccuracies in the algorithmic processing of the digital data all contribute to a single generalized noise term. The plane symmetry group and projected Laue class [1,3] (or 2D Bravais lattice type [4]) that is "anchored" to the least broken symmetries [1] are identified as genuine in the presence of generalized noise. More severely broken symmetries that are not anchored in this sense are identified as pseudosymmetries.

Objective symmetry classifications/quantifications have been undertaken for three concentric regions of the electron diffraction pattern in Fig. 1. The well-known electron crystallography program CRISP/ELD 2.1 [5] was used for the extraction of the electron diffraction spot intensities in the program's default (primitive lattice indexing) setting. These intensities were exported as *.hke files. Relevant details of the three regions are given in Table I. The numerical results of our point symmetry classifications/quantifications are given in Tables II to IV. For more technical details, discussions, and additional results, see the free on-line material [6,7]. With a reduced number of electron diffraction spots, one expects that both the normalized sum of squared residuals (N-SSR) and the traditional R_{sym} values acquire lower numbers/percentages, as observed in these three tables. The R_{sym} [5] values identify the least broken point symmetry group for regions A and C correctly, but not the point group that the digital data actually supports best in the information-theoretic (or any other researcher independent) sense for region B.

The key results of our study (and our scientific progress with respect to relying on the traditional R_{sym} values for classifications of electron diffraction spot patterns into point symmetry groups) are given in the third and fourth columns of these tables for the three concentric regions of the electron diffraction pattern in Fig. 1. These are the geometric Akaike Information Criterion (G-AIC) values (which are model-selection bias-corrected residuals [1,3]) and the geometric Akaike weights (which are the probabilities that geometric models with certain oriented-site/point symmetries are the Kullback-Leibler (K-L) best representation of the experimental data within a set of alternative geometric models [2,3] adding up to 100%). For region B, point symmetry *2mm* is the K-L best group, featuring the highest geometric Akaike weight. The average confidence level [1] for preferring point symmetry *2mm* over its three maximal subgroups is 38.83%. Both of the information-theoretic symmetry deviation quantifiers allow not only for objective point symmetry classifications in the presence of generalized noise and pseudosymmetries but also for their quantifications. Tables II to IV illustrate the high sensitivity of our

point group classifications/quantifications to the selected concentric regions of the electron diffraction pattern in Fig. 1.

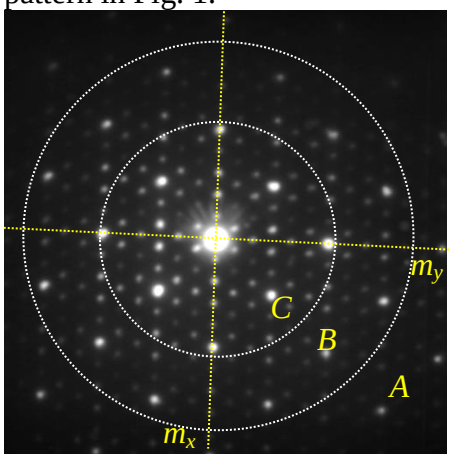

Figure 1. Experimental electron diffraction spot pattern from [5]. The quasi-horizontal mirror line is m_y (*..m*) and its quasi-vertical counterpart is m_x (*.m.*). Very low intensity spots are not readily visible as this is an 8-bit dynamical range pattern.

*.hke file restriction details	Region A	Region B	Region C
Minimal d-spacing in Å (nominal Abbe resolution)	0.85	1.25	2.03
Spot intensity at minimal d-spacing	5.2	6.4	23.8
Total # of spots	436	256	108
Laue indices for minimal d-spacing	$(11,3)_{primitive}$ and $(11,17)_{centered}$	$(5,5)_{primitive}$ and $(5,15)_{centered}$	$(4,-6)_{primitive}$ and $(4,-8)_{centered}$

Table 1. Relevant details on the selected three concentric regions.

It is clear from our analysis that the electron diffraction pattern in Fig. 1 does not feature a hexagonal point symmetry group [6,7]. The apparent hexagonal symmetry of the reciprocal lattice nodes in Fig. 1 is, thus, only a strong translational pseudosymmetry [8] (as confirmed by neutron and X-ray diffraction results) [9]. The diffraction pattern needs, accordingly, to be re-indexed for a rectangular-centered lattice, see last row in Table 1.

Site symmetry of model	N-SSR	G-AIC value (bit)	Geometric Akaike weight (%)	R_{sym} (%)
2	1.18815117	2.277461629	20.37217561	19.2
.m.	0.544655229	**1.633965687**	**28.10417102**	13.2
..m	0.7914292076	1.880739666	24.84188179	14.9
2mm	1.261740485	1.806395714	25.78268098	20.0
6	9.633251966	9.996355452	0.4294384378	56.3
6mm	9.635775834	9.817327577	0.4696521593	56.2

Table 2. Results for region A, K-L best point group *.m.* in bold font.

Site symmetry of model	N-SSR	G-AIC value (bit)	Geometric Akaike weight (%)	R_{sym} (%)
2	0.8774512281	2.133316644	20.72312299	15.1
.m.	0.5001790517	1.756044468	25.02527259	11.7
..m	0.5093608102	1.765226226	24.9106479	11.3
2mm	0.9418990621	**1.56983177**	**27.46720003**	15.9

https://doi.org/10.1017/S1431927622009552 Published online by Cambridge University Press

6	8.013230141	8.431851947	0.8886804812	52.3
6mm	8.016578923	8.225889826	0.9850760216	52.2

Table 3. Results for region B, K-L best point group *2mm* in bold font.

Site symmetry of model	N-SSR	G-AIC value (bit)	Geometric Akaike weight (%)	R_{sym} (%)
2	0.4362919888	0.847183493	22.21634502	13.6
.m.	0.3245002274	0.7353917316	23.49350878	11.1
..m	0.2054457521	**0.6163372563**	**24.93447537**	8.5
2mm	0.4831189841	0.6885647362	24.05006403	14.2
6	4.994388369	5.131352204	2.608418046	46.0
6mm	4.995938079	5.064419997	2.697188755	46.0

Table 4. Results for region C, K-L best point group *..m* in bold font.

Our point symmetry quantification study of an electron diffraction spot pattern is highly topical because a novel contrast mechanism for 4D scanning transmission electron microscopy (STEM) was recently demonstrated by other authors [10]. That contrast mechanism relies on crystallographic point/site symmetries being treated as continuous features. Their method employs, however, a classifier for point symmetries [11] that has no objective way of dealing with the hierarchical aspects [12] of these symmetries, i.e. the well-known point symmetry inclusion relationships. Their classifier has also no inbuilt feature to distinguish between genuine symmetries and pseudo-symmetries in experimental data.

Our point symmetry quantification method overcomes both of these shortcomings at once and is, therefore, poised to make a contribution to the future refinement of the novel [10] imaging mode for 4D STEM imaging with fast pixilated detectors. With an almost parallel scanning nano-beam, one can expect a high sensitivity of the information-theoretic point symmetry quantifiers for different locations within a crystal's unit cell. A high sensitivity to minute symmetry changes will make the new STEM contrast mode more useful [13].

References:

[1] P Moeck, Acta Cryst. A **78**, 2022, in print, doi: 10.1107/S2053273322000845 & expanded version arXiv: 2108.00829, 35 pages, Feb. 2022.
[2] A Dempsey and P Moeck, arXiv: 2009.08539, 74 pages, Dec. 15, 2020.
[3] P Moeck, Symmetry **10** (2018), p. 133, (open access).
[4] P Moeck in "Microscopy and Imaging Science: Practical Approaches to Applied Research and Education", ed. A. Méndez-Villas, (Badajoz: FORMATEX, 2017) p. 503 & arXiv: 2011.13102.
[5] X Zou, S Hovmöller, and P Oleynikov, Electron Crystallography: Electron Microscopy and Electron Diffraction, (Oxford University Press, 2011).
[6] P Moeck and L von Koch, arXiv: 2201.04789, 4 pages, Jan.-Feb. 2022.
[7] P Moeck and L von Koch, arXiv: 2202.00220, 4 pages, Feb. 2022, submitted to 22nd Intern. Conf. Nanotech., July 4 - 8, 2022, Palma de Mallorca, Spain.
[8] P Moeck and P DeStefano, Adv. Struct. and Chem. Imaging **4** (2018), p. 5 (open access).
[9] V G Zubkov, et al., J. of Alloys and Comp. **203** (1994), p. 209.
[10] M Krajnak and J Etheridge, PANS **117** (2020), p. 27805.
[11] T Masuda, et al., Pattern Recogn. **26** (1993), p. 1245.

https://doi.org/10.1017/S1431927622009552 Published online by Cambridge University Press

[12] K Kanatani, IEEE Trans. Pattern Anal. Machine Intellig. **19** (1997), p. 246.
[13] Our numerical results were calculated from $*$.hke files by programs that the second author of this paper, Lukas von Koch, wrote. This work was supported by a Faculty Enhancement Grant from Portland State University to the first (and corresponding) author.

https://doi.org/10.1017/S1431927622009552 Published online by Cambridge University Press